論 文
36~10~3

이상적이지 않은 직류변환기의 상태공간 모델링(Ⅰ)

A State-Space Modeling of Non-Ideal DC-DC Converters (Ⅰ)

林 春 澤*·鄭 圭 範*·曺 圭 亨**
(Chun-taek Rim, Gyu-bum Joung, Gyu-hyeong Cho)

ABSTRACT

A new method for the modeling of non-ideal dc-dc converters whose switching times are finite is proposed. The effects of finite turn-on, turn-off times, delay time, storage time, reverse recovery process on the system stability, dc transfer function and efficiency are investigated. It is verified how system poles are changed and how dc transfer function and efficiency are decreased by non-ideal switching.

INTRODUCTION

The modeling of the network which contains switches has drawn much attention because of the unusual properties of switches in comparison with other circuit elements. This is the reason why there are so many modelings in the power electronics which are not found in other fields.

The difficulties in the modeling of the switched network are mainly due to the non-linear and time-varying nature of the switch. Furthermore the mechanism of the switching system is far different from an ordinary system. Fig. 1 shows this difference. By switching the topology of network is changed and the system matrices A, B, C and D are, therefore, changed. So to control the output of the switching system the ststem matrices must be varied by switches instead of the source as done in the ordinary system. This results in the non-linear and time-varying. The source in the switching system is considered as the disturbance in many cases.

To convert this non-liner time-varying problem to an easier form there have been a few attempts. A feasble method is the state-space average modeling, which averages out the time-varying term and perturbs the non-linear term to obtain an LTI(Linear Time-Invariant)

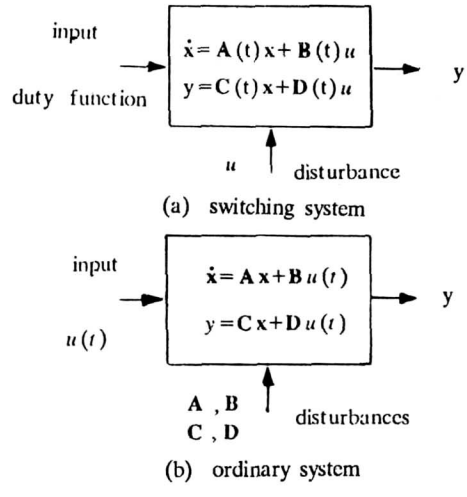

Fig.1. Comparison of systems.

*正 會 員：韓國科學技術院 電氣 및 電子科 博士課程
**正 會 員：韓國科學技術院 電氣 및 電子科 副教授·工博
接受日字：1987年 1月27日
1次修正：1987年 8月20日
2次修正：1987年 9月23日

expresion. 1) This modeling is applicable only when the switch is nearly ideal. A recent work, the fast switch modeling is applicable to the non-ideal switching case. 2) However the output filter of the switching system is assumed to be ideal in the fast switch modeling. The system dynamics can not be explained by this modeling. So far, there has been no exact modeling suit for high frequency or high power applications where the switching time is important. [3), 4)]

A new modeling which is believed to be very suitable for this case is presented in this paper. Neither the output filter nor the switch needs to be ideal. Switchs are described by switching functions and a state equation is set up with them. Then the resultant state equation is averaged and perturbed. The proposed modeling procedure is explained for boost converter case, however it is also possible to apply this modeling technique to all dc-dc converters such as buck and buck-boost converters.

MODELING PROCEDURE

It is assumed that all passive elements are LTI, however, no switch is assumed to be LTI and ideal. The converter is also assumed to be operated in the continuous conduction mode. Fig. 2 and Fig. 3 show the circuit to be modeled and its switching waveforms respectively.

A. Exact State-Space Model

In order to derive a state equation, states x_1, x_2 are allocated to the current of the inductor L and the voltage of the capacitor C. Then the derivatives of the states are expressed as the functions of the states, source and circuit parameters:

$$L\dot{x}_1 = u - R_s x_1 - v \tag{1a}$$

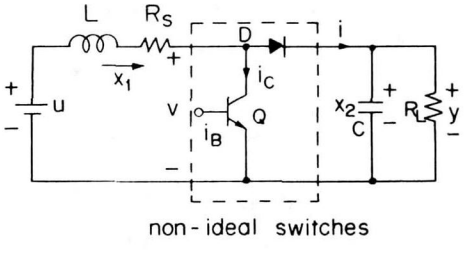

Fig.2. Boost converter.

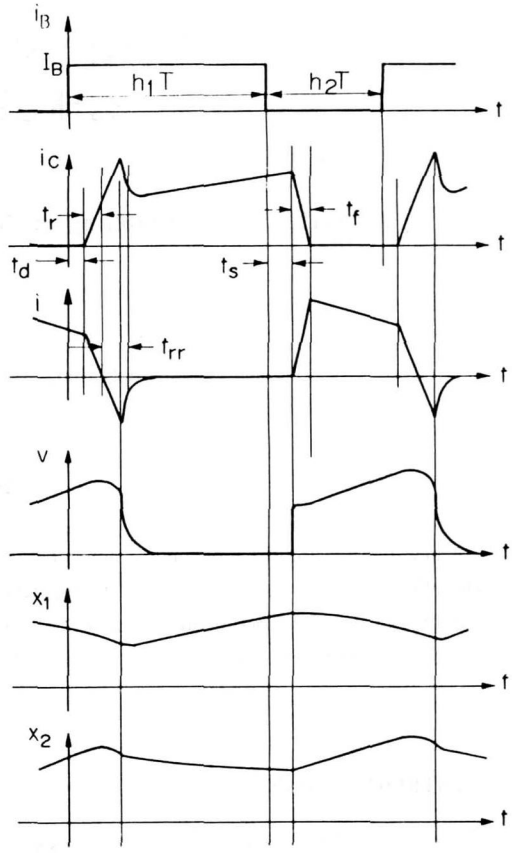

Fig.3. Switching waveforms of boost converter.

$$C\dot{x}_2 = i - \frac{x_2}{R_L} \tag{1b}$$

Note that this state equation is also valid for the non-ideal switch case as well as the ideal switch case. What is rematined is to express v and i as the functions of already known variables. From the switching waveforms we can observe that these are the switched portions of the x_2 and x_1, respectively. So they can be represented as follows:

$$v = s_1(t)x_2, \quad i = s_2(t)x_1 \tag{2}$$

where $s_1(t)$ and $s_2(t)$ are defined as the switching functions and given by

$$s_1(t) = \frac{v}{x_2}, \quad s_2(t) = \frac{i}{x_1} \tag{3}$$

Fig. 4 shows these switching functions. Provided that

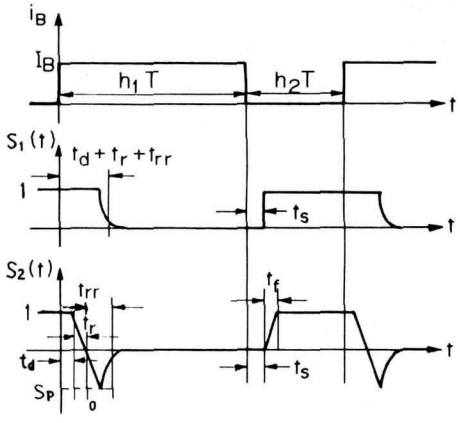

Fig.4. Switching tunctions $s_1(t)$ and $s_2(t)$.

the switching times are known then the switching functions are fully determined. Substituting eq. 2 to eq. 1 the state equation and the output equation of the boost converter are obtained.

$$\begin{bmatrix}\dot{x}_1\\ \dot{x}_2\end{bmatrix}=\begin{bmatrix}-\frac{R_s}{L}-\frac{s_1(t)}{L}\\ \frac{s_2(t)}{C}-\frac{1}{CR_L}\end{bmatrix}\begin{bmatrix}x_1\\ x_2\end{bmatrix}+\begin{bmatrix}\frac{1}{L}\\ 0\end{bmatrix}u \tag{4a}$$

$$y=[\,0\quad 1\,]\begin{bmatrix}x_1\\ x_2\end{bmatrix} \tag{4b}$$

Eq. 4 is of the form

$$\dot{x}=A(t)x+Bu \tag{5a}$$

$$y=Cx \tag{5b}$$

Note that the exact model of the converter is time-varying form, which is the general property of the switching system. This exact model can be used for simulation.

B. State-Space Averaging and Perturbation

To eliminate the time-varying term in the matrices **A**(t), **B**(t), and **C**(t), averaging is taken for the matrices. A general state space averaged expression is as follows:

$$\dot{x}=\bar{A}x+\bar{B}u \tag{6a}$$

$$y=\bar{C}x \tag{6b}$$

where

$$\bar{A}=\frac{1}{T}\int_0^T A(t)\,dt,\quad \bar{B}=\frac{1}{T}\int_0^T B(t)\,dt$$

$$\bar{C}=\frac{1}{T}\int_0^T C(t)\,dt \tag{7}$$

In the boost converter case, the matrices are evaluated as follows:

$$\bar{A}=\begin{bmatrix}-\frac{R_s}{L} & -\frac{s_1}{L}\\ \frac{s_2}{C} & -\frac{1}{CR_L}\end{bmatrix},\quad \bar{B}=B=\begin{bmatrix}\frac{1}{L}\\ 0\end{bmatrix}$$

$$\bar{C}=C=[\,0\quad 1\,] \tag{8}$$

The s_1 and s_2 are the averages of $s_1(t)$ and $s_2(t)$ respectively. They are evaluated from Fig. 4 as follows:

$$s_1=\frac{1}{T}\int_0^T s_1(t)\,dt=1-h+t_1 f \quad \text{for } H_{min}<h<H_{max} \tag{9a}$$

$$s_2=\frac{1}{T}\int_0^T s_2(t)\,dt=1-h+t_2 f \quad \text{for } H_{min}<h<H_{max} \tag{9b}$$

where

$$h=h_1=1-h_2,\ t_1=t_d+t_r+t_{rr}-t_s,$$
$$t_2=t_d+\frac{t_r}{2}-\tau-t_s-\frac{t_f}{2}$$
$$f=\frac{1}{T},\ H_{min}=(t_d+t_r+t_{rr})/T,\ H_{max}=1-(t_s+t_f)/T \tag{10}$$

t_d: turn on delay time, t_r: rise time, t_s: storage time, t_f: turn off time, t_{rr}: reverse recovery time

The H_{min} and H_{max} are determined by the switch turn-on / off overlap condition. Assuming that the diode reverse recovery charge Q_{rr} is proportional to its forward current, then Q_{rr} can be rewritten as fllows by introducting a new variable τ:

$$Q_{rr}=-\int_0^{t_{rr}} i_D(t)\,dt=-\int_0^{t_{rr}} i_L(t)\,s_2(t)\,dt$$
$$\cong -i_L(t)\frac{s_\rho t_{rr}}{2}$$
$$=\tau i_L(t)$$
$$\text{or}\quad \tau=-\frac{s_\rho t_{rr}}{2} \tag{11}$$

The inductor current $i_L(t)$ has been assumed to be constant and τ is found to be the life time of the minority carrier. Now eq. 6 is of the form

$$\dot{x}=A(h)x+B(h)u \tag{12a}$$

$$y = C(h)\,x \tag{12a}$$

To eliminate the non-linearity in eq. 12 the matrices are expanded in power series as

$$A(h) = A(H_0) + \frac{\partial A(h)}{\partial h}\bigg|_{h=H_0}(h-H_0) + \cdots \cong A_0 + A_1(h-H_0) \tag{13a}$$

$\mathbf{B}(h)$ and $C(h)$ are expanded similar to $\mathbf{A}(h)$ as

$$B(h) = B_0 + B_1 \cdot (h-H_0) \tag{13b}$$

$$C(h) \cong C_0 + C_1 \cdot (h-H_0) \tag{13c}$$

Substituting eq. 13 to eq. 12 and taking the following perturbations

$$h = H_0 + \hat{h},\ x = X_0 + \hat{x},\ y = Y_0 + \hat{y} \tag{14}$$

we obtain

$$(\dot{X}_0 + \dot{\hat{x}}) = (A_0 + A_1\hat{h})(X_0 + \hat{x}) + (B_0 + B_1\hat{h})U_0$$
$$(Y_0 + \hat{y}) = (C_0 + C_1\hat{h})(X_0 + \hat{x}) \tag{15}$$

In eq. 15 input u is assumed to be constant and is not perturbed. Ignoring the bilinear term $\hat{h}\hat{x}$, eq. 15 is separated into the dc and the ac equations as follows:

$$\dot{X}_0 = A_0X_0 + B_0U_0$$
$$Y_0 = C_0X_0 \tag{16}$$

and

$$\dot{\hat{x}} = A_0\hat{x} + (A_1X_0 + B_1U_0)\hat{h}$$
$$\hat{y} = C_0\hat{x} + C_1X_0\hat{h} \tag{17}$$

From eq. 16, the operating point Y_0 can be evaluated by setting $\dot{X}_0$ to zero as

$$A_0X_0 + B_0U_0 = 0 \tag{18a}$$

$$Y_0 = -C_0A_0^{-1}B_0U_0 \tag{18b}$$

From eq. 17 the ac transfer function $G(s)$ can be obtained as

$$G(s) = \frac{\hat{Y}(s)}{\hat{H}(s)} = C_0(sI - A_0)^{-1}(A_1X_0 + B_1U_0) + C_1X_0 \tag{19}$$

We can check the system stability by examining the characteristic equation

$$|sI - A_0| = 0 \tag{20}$$

In the boost converter case, these matrices, $\mathbf{A}_0$, $\mathbf{A}_1$, $\cdots$, $\mathbf{C}_1$ are found to be as follows:

$$A_0 = \begin{bmatrix} -\frac{R_s}{L} & -\frac{1-H_0+t_1f}{L} \\ \frac{1-H_0+t_2f}{C} & -\frac{1}{CR_L} \end{bmatrix},$$

$$A_1 = \begin{bmatrix} 0 & \frac{1}{L} \\ -\frac{1}{C} & 0 \end{bmatrix},\quad B_0 = \begin{bmatrix} \frac{1}{L} \\ 0 \end{bmatrix},\quad B_1 = 0$$

$$C_0 = [\,0\quad 1\,],\quad C_1 = 0 \tag{21}$$

C. Pole Frequency Deviation Effect

Now let's investigate the effect of non-ideal switches on the pole frequency. Considering that the s_1 and s_2 of eq. 9 are $1-h+t_1f$ and $1-h+t_2f$ respectively, we can see that duty cycles are changed from h's to $h-t_1f$, $h-t_2f$ by non-ideal switching. Then we can investigate the duty cycle variation effect on the pole frequency to see open loop system stability. Applying eq. 21 to eq. 20, we obtain

$$s^2 + \left(\frac{R_s}{L} + \frac{1}{CR_L}\right)s + \frac{(1-H_0+t_1f)(1-H_0+t_2f) + R_s/R_L}{LC} = s^2 + 2\zeta\omega_n s + \omega_n^2 = 0 \tag{22}$$

The normalized natural frequency ω_n^* and damping factor ζ^*, which are the ratios of the practical ones in relation to the ideal ones with zero duty factor are given by

$$\omega_n^* = \frac{\omega_n}{\omega_n|_{t_1,\,t_2,\,H_0=0}} = \sqrt{\frac{R_s/R_L + (1-H_0+t_1f)(1-H_0+t_2f)}{R_s/R_L + 1}} \tag{23a}$$

and

$$\zeta^* = \frac{\zeta}{\zeta|_{t_1,\,t_2,\,H_0=0}} = \sqrt{\frac{R_s/R_L + 1}{R_s/R_L + (1-H_0+t_1f)(1-H_0+t_2f)}} = \frac{1}{\omega_n^*} \tag{23b}$$

The ω_n^* and ζ^* are plotted in Fig. 5 for a typical power switching transistor whose current level is several tens of amperes. In fact the switching parameters are a function of collector current, however, they are assumed to

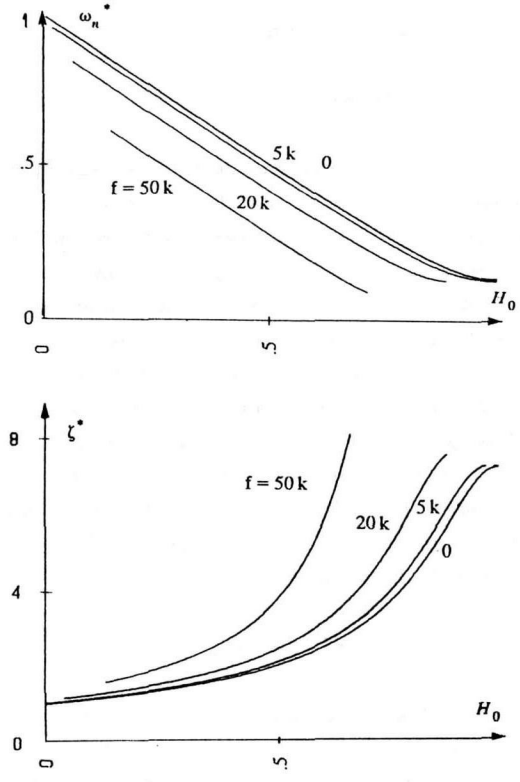

Fig.5. Pole frequency deviations.

be constant for illustration purpose. The switching times and resistances selected in this paper are as follows:

$t_d=0.2\mu s$, $t_r=0.6\mu s$, $t_{rr}=2\mu s$, $t_s=5\mu s$, $t_f=0.8\mu s$, $\tau=2\mu s$ (24a)

$t_1=-2.2\mu s$, $t_2=-6.9\mu s$, $R_s=1ohm$, $R_L=50ohms$ (24b)

We can see that the damping factor increases as a function of switching frequency. Therefore we can conclude that the practical switch increases system stability and this effect becomes dominant as the switching frequency increases. This fact may not be true for some switches where the values t_1 and t_2 are quite different from those used in this paper. However, in practice, the result obtained in this paper is true since t_s is much larger than other switching times and t_1, t_2 are roughlyt$_s$.

D. DC Transfer Function Deviation Effect

To check the effect of the non-ideal switch on the dc-transfer funcition, eq. 18b is evaluated using eq. 21. The dc-transfer function G_{dc} is then

$$G_{dc}=\frac{Y_0}{U_0}=-C_0A_0^{-1}B_0 = \frac{(1-H_0+t_2f)}{\frac{R_s}{R_L}+(1-H_0+t_1f)(1-H_0+t_2f)} \quad (25)$$

Fig. 6 shows the dc transfer function as a function of duty factor for several different switching frequencies.

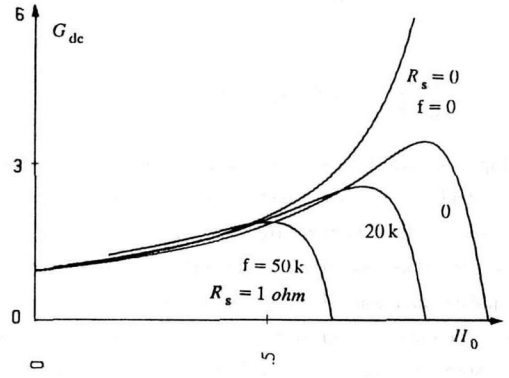

Fig.6. DC transfer function degeneration.

The switching times and resistances used here are the same as those given in eq.24.Note that the practical boost converter has the maximum dc gain less than infinite. This is mainly due to the inductor resistance R_s.

The maximum dc gain occurs at the point H_0^* given as

$$\frac{\partial G_{dc}}{\partial H_0}\Big|_{H_0=H_0^*}=0$$

$$\text{or } H_0^*=1-\sqrt{\frac{R_s}{R_L}}+t_2f \quad (26)$$

And the maximum value is as follows:

$$G_{dc}(H_0^*)=\frac{1}{2\sqrt{\frac{R_s}{R_L}}+(t_1-t_2)f} \quad (27)$$

E. The Efficiency Degeneration Effect

The efficiency η of the boost converter can be evaluated by comparing the input and output powers. It is assumed that the converter has no ripple.

$$\eta = \frac{P_o}{P_i} = \frac{V_c^2/R_L}{U_0 I_L} \tag{28}$$

Evaluating $\mathbf{X}_0$ from eq. 18a we can find out the V_c and I_L. Substituting these to eq. 28 the efficiency is obtained as

$$\eta = \frac{(1-H_0+t_2 f)^2}{R_s/R_L + (1-H_0+t_1 f)(1-H_0+t_2 f)} \tag{29}$$

To concentrate our attention to switching effect the inductor resistance R_s is set to zero. Then the efficiency η becomes

$$\eta = \frac{V_c^2/R_L}{U_0 I_L}\bigg|_{R_S=0} = \frac{1-H_0+t_2 f}{1-H_0+t_1 f} \tag{30}$$

Fig. 7 shows the efficiency degeneration effect by the non-ideal switch as a function of switching frequency for several duty factors. Remark on the fact that the efficiency does not decrease linearly as the switching frequency increases. This is due to the interaction between the output filter and the switch. Those who want to determine the maximum switching frequency for guaranteeing the efficiency may use this corrected curve instead of rough calculation.

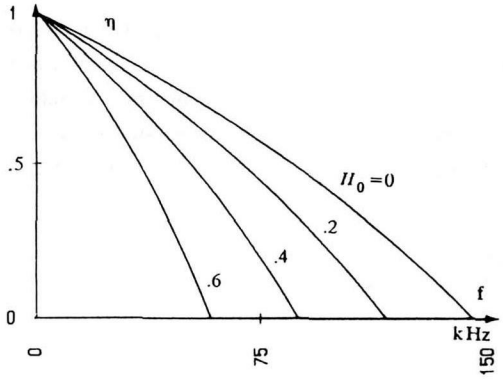

Fig.7. Efficiency degeneration

CONCLUSION

The extension and generalization of the state-space average modeling to the non-ideal switching case has been performed. Stability of boost converter is improved by the non-ideal switching. DC gain is degenerated and it is identified that a maximum dc gain point which depends on the load and source resistances and switching frequency exists. The efficiency does not decrease, however, linearly as a function of switching frequency.

The extension of this modeling to the discontinuous conduction mode case may be possible. And switching parameter variation by current or voltage may be taken into account if detail solution is required. These are remained for further works.

REFERENCE

1) R. D. Middlebrook and S. Cuk, "A general unified approach to modeling switching converter stages," in *IEEE Power Electronics Specialists Conf. Rec.*, 1977, pp. 36-57

2) G. eggers, "Fast switches in linear networks", *IEEE Trans. Power electronics* Electronics, Vol PE-1, No. 3, pp. 129-140, July 1986.

3) Khai D. T. Ngo, "Low frequency characterization of PWM converter", *IEEE Trans. Power Electronics*, Vol. PE-1, No. 4, pp. 223-230, October 1986.

4) W. M. Polivka, P. R. K. Chetty and R. D. Middlebrook, "State-space average modelling of converters with parasitics and storage-time modulation", in *IEEE Power Electronics Specialists Conf. Rec.*, 1980, pp. 219-243.